Palmatine suppresses glutamine-mediated interaction between pancreatic cancer and stellate cells through simultaneous inhibition of survivin and COL1A1

Divya Chakravarthy[a], **Amanda R. Muñoz**[a], **Angel Su**[a], **Rosa F. Hwang**[g], **Brian R. Keppler**[h], **Daniel E. Chan**[d], **Glenn Halff**[e], **Rita Ghosh**[a,b,c], and **Addanki P. Kumar**[a,b,c,f,*]

[a]Department of Urology, University of Texas Health San Antonio, San Antonio, TX 78229, USA

[b]Department of Pharmacology, University of Texas Health San Antonio, San Antonio, TX 78229, USA

[c]Department of Molecular Medicine, University of Texas Health San Antonio, San Antonio, TX 78229, USA

[d]Division of Medical Oncology, CU Denver, USA

[e]Department of Transplant Surgery, University of Texas Health San Antonio, San Antonio, TX 78229, USA

[f]Audie Murphy South Texas Veterans Health Care System, San Antonio, TX 78229, USA

[g]Department of Surgical Oncology, The University of Texas MD Anderson Cancer Centre, Houston, TX 77030, USA

[h]Metabolon, Inc., 617 Davis Drive, Suite 400, Morrisville, NC 27560, USA

Abstract

Reciprocal interaction between pancreatic stellate cells (PSCs) and cancer cells (PCCs) in the tumor microenvironment (TME) promotes tumor cell survival and progression to lethal, therapeutically resistant pancreatic cancer. The goal of this study was to test the ability of Palmatine (PMT) to disrupt this reciprocal interaction *in vitro* and examine the underlying mechanism of interaction. We show that PSCs secrete glutamine into the extracellular environment under nutrient deprivation. PMT suppresses glutamine-mediated changes in GLI signaling in PCCs resulting in the inhibition of growth and migration while inducing apoptosis by inhibition of survivin. PMT-mediated inhibition of (glioma-associated oncogene 1) GLI activity in stellate cells leads to suppression (collagen type 1 alpha 1) COL1A1 activation. Remarkably, PMT potentiated gemcitabine's growth inhibitory activity in PSCs, PCCs and inherently gemcitabine-resistant pancreatic cancer cells. This is the first study that shows the ability of PMT to inhibit growth of

*Corresponding author. Department of Urology, University of Texas Health San Antonio, 8403 Floyd Curl Drive, San Antonio, TX 78229, USA. kumara3@uthscsa.edu (A.P. Kumar).

PSCs and PCCs either alone or in combination with gemcitabine. These studies warrant additional investigations using preclinical models to develop PMT as an agent for clinical management of pancreatic cancer.

Keywords

GLI signaling; Palmatine; Pancreatic cancer; Desmoplasia; glutamine

1. Introduction

Late stage diagnosis and lack of early detection markers contribute to the near equal rates of pancreatic cancer incidence and mortality. 20% patients are eligible for surgical resection and 3–4% remain disease-free following surgical resection while about 80% will relapse and die of the disease [1]. Gemcitabine (GEM)-monotherapy has been the standard of care for advanced pancreatic ductal adenocarcinoma (PDAC) for more than a decade although overall survival of patients on GEM is an average of 6 months. Therapeutic approaches based on combination of GEM with additional chemotherapy agents such as oxaliplatin, irinotecan, leucovorin and 5-FU (FOLFIRINOX) have provided modest survival benefit with significant toxicity, and is reserved for a select group of patients [2]. Therefore, there is a critical need for new agents that can effectively manage PDAC.

Uniquely, a dense stroma or desmoplastic reaction (DR) in the tumor microenvironment (TME) plays a critical role in tumor maintenance and in limiting therapeutic efficacy by decreasing drug delivery [3,4]. This constitutes about 90% of the tumor area and is comprised of a variety of cells including stellate cells (PSCs), fibroblasts, endothelial cells, myeloid cells, and extracellular matrix (ECM) components such as collagens [5]. PSCs, considered to be the driver of pancreatic fibrosis, are usually quiescent in the normal pancreas, but can be activated by a number of factors including inflammation. Once activated, these cells exhibit a myofibroblastic phenotype including expression of alpha smooth muscle actin (α-SMA), and collagen 1 type 1 alpha 1 (COL1A1) [6]. Pancreatic cancer cells (PCCs) also activate PSCs in a paracrine fashion by secreting a variety of cytokines and growth factors including Sonic hedgehog (SHH). Such paracrine interactions between PSCs and PCCs promote tumor progression by regulating a plethora of oncogenic processes including proliferation, migration, invasion and apoptosis of cancer cells [7-10].

Given the importance of DR in tumor progression and therapeutic resistance, our goal is to develop a strategy for PDAC using agents that inhibit growth of activated PSCs and PCCs as well as their synergistic interactions in the TME. In this study, we report the potential utility of palmatine (PMT) to inhibit growth of PSCs, PCCs and PSC-PCC interaction using *in vitro* models.

2. Materials and methods

2.1. Cell lines and chemicals

Human pancreatic cancer cell lines HPNE, MIA PaCa-2, CFPaC-1 and PANC-1 were obtained from ATCC (Rockville, MD). PSCs (obtained from Dr. Rosa, Hwang, UT MD

Anderson Cancer Center, Houston, TX) and PANC-1 cells were cultured in DMEM medium (Mediatech, Inc., Manassas, VA) supplemented with 10% fetal bovine serum (FBS), 100-μg/mL penicillin-streptomycin, and 100-μg/mL amphotericin. HPNE, HPNE-Ras, and MIA PaCa-2 cells were maintained as previously described [11-13]. Palmatine (PMT) was obtained from LKT Laboratories Inc. (St Paul, MN) and all other chemicals were analytical grade.

2.2. Metabolomic profiling

PSCs were treated with 5 mM and 25 mM glucose under serum free conditions with 5 and 25 mM mannitol used as osmotic controls. After 24 or 48 h of incubation, the cell supernatants were harvested; flash frozen for use in metabolomic profiling performed by Metabolon, Inc. (Durham, NC) using standard protocols.

2.3. Biochemical experiments

Cell proliferation was measured 24 and 48 h of incubation with PMT (10, 25, 50, 75, 100, 150 and 200 μg/mL) using CellTiter 96 Aqueous One solution assay (Promega Corporation, Madison, WI) as described previously [11,12]. Apoptosis was measured using Annexin V Apoptosis Detection Kit APC (eBioscience, Inc., San Diego, CA) following treatment with PMT (30 h) as per manufacturer's instructions. Etoposide (Etop) was used as a positive control. Colony forming ability was determined using crystal violet staining. Cell invasion assay was performed according to the manufacturer's instructions (ECM556, Chemicon, EMD Millipore, Billerica, MA). Immunoblot analysis, Real-Time PCR and transient expression assays were conducted as described previously using either chemiluminescence or Infrared Imaging [11-13].

2.4. Statistics and ethics statement

All experiments were repeated at least 3 times using either duplicate or triplicate samples. Statistical significance was determined by two-way ANOVA or student's t-test. Results were considered significant if the p value < .05.

3. Results

3.1. Palmatine inhibits sonic hedgehog pathway and growth of pancreatic stellate cells

Published studies from our laboratory identified palmatine (PMT) as a hydrophilic compound with potential with antitumorigenic activity [14,15]. PMT is one of the biologically active components of Nexrutine® which was reported to reduce fibrosis in an inflammation-driven pancreatic cancer mouse model (BK5-Cox-2) [11]. Since Hh signaling is active in both stroma and tumor cells and because GLI plays an important role in tumor-stromal interaction, we examined the effect of PMT on the expression of Hh effector molecules, GLI1 and GLI2. GLI reporter activity and downstream targets including COL1A1, which is involved in collagen deposition and plays a critical role in aggressive behavior of PDAC was also examined. PMT treatment (48 h) decreased the expression and protein levels of GLI1 and GLI2 in PSCs (Figs. 1A and B and protein levels of GLI1 and GLI2 in PSCs; quantification data shown in S1A and B). A decrease in GLI reporter activity was also seen in response to PMT treatment (Fig. 1C). PMT-mediated decreased reporter

activity was reflected by the decrease in message and protein levels of downstream targets: PTCH1 (patched 1), IκBKE (inhibitor of nuclear factor kappa-B kinase subunit epsilon) and COL1A1 (collagen type 1 alpha 1 chain; Figs. 1D and E; quantification data shown in S1C-E). Inhibition of GLI1 and GLI2 using RNAi inhibited COL1A1 message suggesting that PMT reduces COL1A1 via GLI (Fig. 1F). These results taken together suggest that PMT inhibits SHH pathway in PSCs.

To determine the biological significance of these observations we determined the effect of PMT on cellular homeostasis by assessing growth, apoptosis, autophagy and invasive potential in PSCs. PMT caused dose-dependent decreases in proliferation and colony forming ability (measured by clonogenic survival assays) in PSCs with ~IC_{50} of 75 μg/mL (Figs. 1G and H). Treatment with PMT significantly reduced mRNA expression and protein levels of survivin (Figs. 1I and J). Despite decreased levels and expression of survivin, we did not observe changes in apoptosis as determined by PARP cleavage or Annexin V staining under these experimental conditions (Figs. 1K and S1F). It is well established that tumors grow in severe hypoxic, nutrient deprived microenvironments and show elevated levels of autophagy [16]. Since there was no significant change in apoptotic cells, we reasoned that PMT might use autophagy to regulate PSC growth. We determined changes in cell survival and turnover of LC3BII following PMT treatment in the presence and absence of chloroquine (CQ). Analysis of these data showed a marginal yet significant decrease in LC3BII turnover suggesting that it is not delivered to lysosome for degradation resulting in decreased autophagy in the presence of PMT (Figs. 1K, S1G, and S1H). Remarkably, PMT inhibited invasive ability of PSCs with no significant effect on migration (Figs. 1L and S1I). Trypan blue viability assessment of PSCs treated with PMT in the presence and absence of CQ corroborated our apoptosis data; that PMT does not induce apoptotic cell death (Fig. S1J). Collectively, these data suggest that PMT is a cytostatic agent with a propensity to inhibit clonogenicity, invasion and possibly autophagy-mediated survival of PSCs.

3.2. Palmatine inhibits growth of pancreatic cancer cells

To determine the effect of PMT on other pancreatic cells, we evaluated its effects on the growth of normal HPNE, mutant KRAS transformed HPNE (HPNE-Ras) cells, and PCC lines: MIA PaCa-2 and PANC-1. HPNE-Ras cells were sensitive to growth inhibitory effects of PMT with IC_{50} values of 50 μg/mL (Fig. 2A; dashed line). In contrast, HPNE cells were comparatively resistant to PMT treatment as doses of 150 μg/mL or greater were required to see growth inhibitory effects (Fig. 2A; solid line and data not shown). Similar to HPNE-Ras cells, PMT-mediated growth inhibitory effects were observed in the cancer cell lines, MIA PaCa-2 and PANC-1 (Figs. 2B and C). PMT reduced the protein levels of GLI2 and PTCH1 in MIA PaCa-2 cells (Figs. 2D, S2A, and S2B). However, we did not observe these effects in PANC-1 cells (Figs. 2D, S2C and S2D). PMT treatment significantly reduced expression and levels of survivin in MIA PaCa-2, but not PANC-1 cells (Figs. 2D and E). Consistent with this observation, PMT treatment induced apoptosis in MIA PaCa-2 and not PANC-1 cells as indicated by the appearance of cleaved PARP and Annexin V staining (Figs. 2D and S3A).

Examination of autophagic activity following PMT treatment showed no significant effect on LC3B cleavage or p62 levels in MIA PaCa-2 and PANC-1 cells (Fig. 2F; quantification data is shown in Figs. S3B and C). Significant decrease in viability and induction of PARP cleavage was observed in MIA PaCa-2 but not in PANC-1 cells when autophagy was inhibited using CQ (Figs. 2F and G). These data suggest that autophagy primarily functions as a cell survival mechanism in these cells, which is consistent with published reports [17]. We believe that inhibition of autophagy using an autophagic inhibitor lowers the autophagic threshold in MIA PaCa-2 cells leading to decreased cell viability and induction of apoptosis (Figs. 2F and G). The effects of PMT on PANC-1 cells are not evident possibly due to a higher autophagic threshold (Fig. 2G right panel). Consistent with this speculation, basal LC3BII levels are significantly higher in PANC-1 compared to MIA PaCa-2 cells (data not shown). Interestingly, PMT marginally inhibited the migratory ability of MIA PaCa-2 cells with no effect on PANC-1 cells. In addition, PMT had no significant effect on invasive ability of PCCs under these experimental conditions (Figs. S3D, S3E, and data not shown). Taken together, these data suggest that PMT inhibits growth of cancer cell lines, albeit differentially possibly depending on the cellular context. It inhibits growth and induces apoptosis in MIA PaCa-2 cells and pharmacological inhibition of autophagy using CQ enhances PMT-induced apoptosis in MIA PaCa-2 cells. Additionally, although PMT reduces growth of PANC-1 cells, they are resistant to apoptosis induction.

3.3. PMT-mediated effects involve secretory factor

Although PSCs have invasive and migratory abilities, in conjunction with PCCs they acquire the ability to invade and migrate in a bi-directional manner [18]. Based on our data, we reasoned that PMT might hinder PSC-PCC communication. Therefore, we examined the migratory ability of PCCs following treatment with conditioned media from PSCs in the absence and presence of PMT (CM and PMTCM respectively). Intriguingly, CM from PSCs enhanced the migratory ability of both MIA PaCa-2 and PANC-1 cells (Fig. 3A and B, S4A, and S4B). Interestingly, PMTCM significantly decreased migratory ability of these cells (Fig. 3C and D, S4C, and S4D). It is noteworthy that PMT alone decreased migratory ability of MIA PaCa-2 cells approximately 20% with no effect on PANC-1 cells (Figs SF3D and SF3E). Intriguingly, CM-mediated enhanced migratory ability of MIA PaCa-2 and PANC-1 cells was associated with increased levels of β-catenin in MIA PaCa-2 cells and SNAIL in PANC-1 cells (Figs. 3E and F, left panel). On the other hand, PMTCM decreased levels of these same markers (Figs. 3E and F, right panel). These results imply the involvement of a secretory factor(s) in mediating PMT-induced effects on migration in cancer cells and that the ability of PMT to inhibit migration of PCCs occurs possibly by reducing the level(s) of such secreted factor(s).

3.4. Palmatine inhibits glutamine-mediated PSC-PCC interaction in vitro

Physiologically tumors grow under hypoxic and nutrient deprived conditions and cancer cells survive in this hostile micro-environment in part through reprogramming their metabolic needs [19]. However, how PSCs growing under such conditions reprogram their metabolic needs to communicate with PCCs to promote their growth and survival remains undefined. To address this, we cultured PSCs in low glucose media (GLM; 5 mM) or glucose-rich media (GRM; 25 mM; generally used in cell culture media) over a time course

of 48 h and performed metabolite analysis using spent media and lysates (for intracellular metabolites). Analysis of metabolite profiling data reveled statistically significant alterations in both secretory (20 upregulated and 40 downregulated) and intracellular biochemicals (44 upregulated and 120 down-regulated) involved in glycolysis, glutamine metabolism and TCA cycle (Table 1; Figs. 4A and B; hierarchical clustering of metabolite data is shown in S5A and B). Specifically, we observed reductions in the secreted levels of glucose, pyruvate and lactate (involved in glycolytic pathway) and significant increases in glutamine and glutamate (involved in glutamine metabolism). Interestingly, the levels of citrate increased while α-ketoglutarate (α-KG) and fumarate decreased with minimal effects on other TCA cycle intermediates (Fig. 4A). This could possibly be due to block in conversion of glutamate to α-KG mediated by glutamate dehydrogenase. Accordingly, we expected to see increased intracellular levels of glutamate. We observed significant decrease in the intracellular levels of biochemicals involved in glycolysis and increase in α-KG and glutamine (Fig. 4B). Box plots showing secreted and intracellular levels of α-KG, glutamate and glutamine are shown in Fig. 5A and B respectively. These data reveal that under low glucose conditions, PSCs utilize alternate carbon sources such as glutamine and glutamate to fuel TCA cycle, which is consistent with published findings [19-22]. These data also indicate that PSCs cultured under reduced glucose conditions secrete significant amounts of glutamine into the extracellular space relative to PSCs growing under glucose enriched conditions, which may facilitate their interaction with PCCs.

To test whether glutamine from PSCs affects PCC biological functions and affects the SHH pathway, we examined the effect of glutamine (GLN) and glucose (GLC) on cancer cell proliferation, migration, and SHH pathway (Fig. 5C–E). MIA PaCa-2 cells supplemented with either glucose or glutamine showed increased proliferation (Fig. 5C) and migration (Fig. 5D) as compared to cells deprived of both glucose and glutamine (Figs. 5C and D). Addition of both glucose and glutamine further increased their proliferation (especially at 48 h) and migration indicating that both glucose and glutamine are involved in increasing proliferation of PCCs (Figs. 5C, D and S5C). Protein levels of GLI1, GLI2, SNAIL, and survivin increased significantly, albeit more prominent at 48 h following supplementation with both glucose and glutamine (Fig. 5E; quantification in S5D). In addition, treatment with PMT reduced the observed changes in the levels of these proteins especially SNAIL and Survivin (Figs. 6A and S5E). Further, under these experimental conditions, PMT inhibited glutamine- or glucose plus glutamine-induced proliferation of cells (Fig. 6B). Glucose, glutamine or combination also enhanced proliferation of liver metastatic CFPaC-1 cells, however, PMT inhibited only glutamine but not glucose or combination-induced proliferation in these cells (Fig. 6C). These findings suggest that PSCs residing in the TME communicate with PCCs in part through glutamine and that glutamine and glucose have growth promoting effects on PCCs (possibly in a cell-specific manner), which is consistent with the published literature [23]. Furthermore, our results show the potential of PMT to disrupt glutamine-mediated effects on PCCs *in vitro*.

3.5. Palmatine works synergistically with gemcitabine to inhibit growth of stellate and cancer cells

It is known that PSCs contribute to therapeutic resistance including GEM resistance by increasing fibrogenesis [1-8]. COL1A1 is involved in GEM resistance and survivin is increased upon treatment with GEM in PCCs [24-26]. These published observations coupled with the ability of PMT to decrease levels of GLI and COL1A1 in PSCs and survivin in cancer cells prompted us to test the hypothesis that PMT may potentiate GEM activity against human PSCs and PCCs. PSCs were treated with increasing concentrations of PMT (0–100 μg/mL) and GEM (0–0.5 μM) as single agents and in combination for 24 h before measuring proliferation. Both PMT and GEM alone or in combination decreased proliferation in a dose dependent manner with IC_{50} of 75 μg/mL for PMT and 0.25 μM for GEM (Fig. S6A). Data generated was subjected to combination index (CI) analyses using the Chou and Talalay method [27]. Isobologram analysis of these data indicate that the combination of PMT and GEM is highly synergistic with CI values reaching less than 0.5 using lower doses of both compounds (0.1 μM GEM plus 25 μg/mL PMT; Fig. 7A). It should be mentioned that single agent dose of 75 μg/mL for PMT and 0.25 μM for GEM is necessary to inhibit proliferation of PSCs by 50%. A similar level of proliferation inhibition was achieved using lower doses of PMT plus GEM (SF6A). We also found that PMT potentiated GEM activity synergistically in MIA PaCa-2, but not PANC-1 cells (Figs. 7B, S6B, and S6C). However, PMT alone inhibited proliferation of PANC-1 cells (Figs. 7C and S6C). Furthermore, we observed a significant decrease in the levels of COL1A1 and survivin in the combination, but not in single agent group (P+G; Fig. 7D; quantification shown in S6D). In preliminary studies, we also observed that PMT decreased the colony forming ability of patient derived pancreatic cancers cells (data not shown). Taken together, these data suggest that PMT alone or in combination with GEM maybe effective against tumor-associated stroma, a major therapeutic barrier as well as pancreatic cancer cells and warrants additional comprehensive investigations to further its clinical development.

4. Discussion

A reason for the high mortality of PDAC and development of GEM resistance could be that most therapeutic strategies are focused on targeting tumor cells alone. In this study, we examined the utility of PMT to inhibit growth of PSCs, PCCs and PSC-PCC interaction using *in vitro* models. Our studies show for the first time that suppressing COL1A1 with the novel hydrophilic agent, PMT, not only inhibits growth of PSCs but also potentiates GEM activity synergistically. PMT treatment affects cell fate by inhibiting growth of pancreatic cancer cells through downregulation of survivin and induction of apoptosis. Remarkably, PMT treatment potentiates GEM-induced growth inhibition in PCCs and inhibits growth of GEM-resistant PCCs. Based on our data we speculate that PMT inhibits GLI mediated activation of COL1A1 and survivin to suppress proliferation and invasion while enhancing sensitivity to GEM. Alternatively, PMT can inhibit PCC-mediated reprogramming of PSCs to secrete glutamine into the extracellular environment thereby preventing PSC-PCC interaction. Experiments using conditioned media and inhibitory effects of PMT on the frequency of colony formation support the possibility that PMT inhibits PSC-PCC interactions (please see hypothetical model in Fig. 8). Additional investigations including

preclinical studies are critical to demonstrate that PMT inhibits direct interaction between PSCs-PCCs.

PSC-secreted COL1A1 can promote invasion and migration of pancreatic cancer cells [28-30]. COL1A1 has also been shown to induce SNAIL and GLI signaling in PCCs [30,31]. Pancreatic cancer cells cultured on organotypic gels consisting of COL1A1, matrigel and stromal cells showed increased expression of β-catenin [32]. The association between survivin and poor prognosis in pancreatic cancer patients is well established and survivin inhibition is known to promote apoptosis and enhance GEM sensitivity [25,26]. Surprisingly we did not observe any evidence for induction of apoptosis despite downregulation of survivin in response to PMT suggesting a role that is independent of apoptosis induction. It is noteworthy to mention that silencing survivin along with XIAP caused partial mesenchymal epithelial transition and enhanced sensitivity to GEM in PANC-1 cells [33]. Increased SNAIL and β-catenin expression in pancreatic tumors was positively associated with lymph node invasion and distant metastasis [34]. Accordingly, it is possible that by down regulating survivin, PMT may influence EMT in PSCs. Given the reports showing that carbon and nitrogen from glutamate can be used to produce proline, which plays a key role in the production of extracellular matrix protein, collagen, we speculate that PMT possibly suppresses COL1A1 via glutamine [21]. Recently, it was shown that PSC-derived alanine functions as an alternative carbon source to support cancer cell growth in the tumor microenvironment [35]. Our observation that glutamine facilitates interaction between PSC-PCC is consistent with these published findings. Our results also demonstrate that PMT augments GEM-induced growth inhibitory activity in PSCs, PCCs and inhibited growth of inherently GEM resistant pancreatic cancer cells. Our findings strongly suggest that PMT alone or in combination with GEM may be beneficial in the clinical management of PDAC. Overall our results suggest PMT is a promising agent and warrants thorough investigations including preclinical testing to establish its use for management of PDAC.

Supplementary Material

Refer to Web version on PubMed Central for supplementary material.

Acknowledgments

References

1. Ryan D, Hong T, Bardeesy N. Pancreatic adenocarcinoma. N Engl J Med. 2014; 371:1039–1049. [PubMed: 25207767]

2. Sclafani F, Iyer R, Cunningham D, Starling N. Management of metastatic pancreatic cancer: current treatment options and potential new therapeutic targets. Crit Rev Oncol Hematol. 2015; 95:318–336. [PubMed: 25921418]

3. Feig C, Gopinathan A, Neesse A, Chan DS, Cook N, Tuveson DA. The pancreas cancer microenvironment. Clin Cancer Res. 2012; 18:4266–4276. [PubMed: 22896693]

4. Duner S, Lopatko Lindman J, Ansari D, Gundewar C, Andersson R. Pancreatic cancer: the role of pancreatic stellate cells in tumor progression. Pancreatology. 2010; 10:673–681. [PubMed: 21242706]

5. Apte M, Pirola RC, Wilson JS. Pancreatic stellate cell: physiologic role, role in fibrosis and cancer. Curr Opin Gastroenterol. 2015; 31:416–423. [PubMed: 26125317]

6. Masamune A, Kikuta K, Watanabe T, Satoh K, Hirota M, Hamada S, Shimosegawa T. Fibrinogen induces cytokine and collagen production in pancreatic stellate cells. Gut. 2009; 58:550–559. [PubMed: 19052021]

7. Vonlaufen A, Phillips PA, Xu Z, Goldstein D, Pirola RC, Wilson JS, Apte MV. Pancreatic stellate cells and pancreatic cancer cells: an unholy alliance. Cancer Res. 2008; 68:7707–7710. [PubMed: 18829522]

8. Bachem MG, Schunemann M, Ramadani M, Siech M, Beger H, Buck A, Zhou S, Schmid-Kotsas A, Adler G. Pancreatic carcinoma cells induce fibrosis by stimulating proliferation and matrix synthesis of stellate cells. Gastroenterology. 2005; 128:907–921. [PubMed: 15825074]

9. Yoshida S, Ujiki M, Ding XZ, Pelham C, Talamonti MS, Bell RH Jr, Denham W, Adrian TE. Pancreatic stellate cells (PSCs) express cyclooxygenase-2 (COX-2) and pancreatic cancer stimulates COX-2 in PSCs. Mol Cancer. 2005; 4:27. [PubMed: 16083499]

10. Bailey JM, Swanson BJ, Hamada T, Eggers JP, Singh PK, Caffery T, Ouellette MM, Hollingsworth MA. Sonic hedgehog promotes desmoplasia in pancreatic cancer. Clin Cancer Res. 2008; 14:5995–6004. [PubMed: 18829478]

11. Gong J, Xie J, Bedolla R, Rivas P, Chakravarthy D, Freeman J, Reddick R, Kopetz S, Peterson A, Wang H, Fischer S, Kumar A. Combined targeting of STAT3/NF-κB/COX-2/EP4 for effective management of pancreatic cancer. Clin Cancer Res. 2014; 20:1259–1273. [PubMed: 24520096]

12. Gong J, Muñoz AR, Pingali S, Payton-Stewart F, Chan DE, Freeman JW, Ghosh R, Kumar AP. Downregulation of STAT3/NF-κB potentiates gemcita-bine activity in pancreatic cancer cells. Mol Carcinog. 2017; 56:402–411. [PubMed: 27208550]

13. Gong J, Muñoz AR, Chan D, Ghosh R, Kumar AP. Stat3 down regulates LC3 to inhibit autophagy and pancreatic cancer cell growth: role of Nexrutine[R]. Oncotarget. 2014; 5:2529–2541. [PubMed: 24796733]

14. Hambright HG, Batth IS, Xie J, Ghosh R, Kumar AP. Palmatine inhibits growth and invasion in prostate cancer cell: potential role for rpS6/NFkappaB/FLIP. Mol Carcinog. 2015; 54:1227–1234. [PubMed: 25043857]

15. Muralimanoharan S, Kunnumakkara A, Shylesh B, Kulkarni K, Haiyan X, Ming H, Aggarwal B, Rita G, Kumar A. Butanol fraction containing berberine or related compound from nexrutine inhibits NFkappaB signaling and induces apoptosis in prostate cancer cells. Prostate. 2009; 69:494–504. [PubMed: 19107816]

16. Ackerman D, Simon MC. Hypoxia, lipids, and cancer: surviving the harsh tumor microenvironment. Trends Cell Biol. 2014; 24:472–478. [PubMed: 24985940]

17. Yang S, Wang X, Contino G, Liesa M, Sahin E, Ying H, Bause A, Li Y, Stommel JM, Dell'antonio G, Mautner J, Tonon G, Haigis M, Shirihai OS, Doglioni C, Bardeesy N, Kimmelman AC. Pancreatic cancers require autophagy for tumor growth. Genes Dev. 2011; 25:717–729. [PubMed: 21406549]

18. Pancreatic, PP. stellate cells and fibrosis. In: Grippo, PJ., HG, M., editors. Pancreatic Cancer and Tumor Microenvironment. Transworld Research Network; Trivandrum (India): 2012.

19. Kimmelman AC. Metabolic dependencies in RAS-driven cancers. Clin Cancer Res. 2015; 21:1828–1834. [PubMed: 25878364]

20. Vander Heiden MG, Cantley LC, Thompson CB. Understanding the Warburg effect: the metabolic requirements of cell proliferation. Science. 2009; 324:1029–1033. [PubMed: 19460998]

21. Altman BJ, Stine ZE, Dang CV. From Krebs to clinic: glutamine metabolism to cancer therapy. Nat Rev Cancer. 2016; 16:619–634. [PubMed: 27492215]

22. Gao P, Tchernyshyov I, Chang TC, Lee YS, Kita K, Ochi T, Zeller KI, De Marzo AM, Van Eyk JE, Mendell JT, Dang CV. c-Myc suppression of miR-23a/b enhances mitochondrial glutaminase expression and glutamine metabolism. Nature. 2009; 458:762–765. [PubMed: 19219026]

23. Son J, Lyssiotis CA, Ying H, Wang X, Hua S, Ligorio M, Perera RM, Ferrone CR, Mullarky E, Shyh-Chang N, Kang Ya, Fleming JB, Bardeesy N, Asara JM, Haigis MC, DePinho RA, Cantley LC, Kimmelman AC. Glutamine supports pancreatic cancer growth through a KRAS-regulated metabolic pathway. Nature. 2013; 496:101–105. [PubMed: 23535601]

24. Armstrong T, Packham G, Murphy LB, Bateman AC, Conti JA, Fine DR, Johnson CD, Benyon RC, Iredale JP. Type I collagen promotes the malignant phenotype of pancreatic ductal adenocarcinoma. Clin Cancer Res. 2004; 10:7427–7437. [PubMed: 15534120]

25. Han Z, Lee S, Je S, Eom CY, Choi HJ, Song JJ, Kim JH. Survivin silencing and TRAIL expression using oncolytic adenovirus increase anti-tumorigenic activity in gemcitabine-resistant pancreatic cancer cells. Apoptosis. 2016; 21:351–364. [PubMed: 26677013]

26. Dong H, Qian D, Wang Y, Meng L, Chen D, Ji X, Feng W. Survivin expression and serum levels in pancreatic cancer. World J Surg Oncol. 2015; 13:189. [PubMed: 26016480]

27. Chou TC, Talalay P. Quantitative analysis of dose-effect relationships: the combined effects of multiple drugs or enzyme inhibitors. Adv Enzym Regul. 1984; 22:27–55.

28. Ikenaga N, Ohuchida K, Mizumoto K, Akagawa S, Fujiwara K, Eguchi D, Kozono S, Ohtsuka T, Takahata S, Tanaka M. Pancreatic cancer cells enhance the ability of collagen internalization during epithelial-mesenchymal transition. PLoS One. 2012; 7:e40434. [PubMed: 22792318]

29. Lu J, Zhou S, Siech M, Habisch H, Seufferlein T, Bachem MG. Pancreatic stellate cells promote hapto-migration of cancer cells through collagen I-mediated signalling pathway. Br J Cancer. 2014; 110:409–420. [PubMed: 24201748]

30. Duan W, Ma J, Ma Q, Xu Q, Lei J, Han L, Li X, Wang Z, Wu Z, Lv S, Ma Z, Liu M, Wang F, Wu E. The activation of b1-integrin by type I collagen coupling with the hedgehog pathway promotes the epithelial-mesenchymal transition in pancreatic cancer. Curr Cancer Drug Targets. 2014; 14:446–457. [PubMed: 24720337]

31. Shields MA, Dangi-Garimella S, Krantz SB, Bentrem DJ, Munshi HG. Pancreatic cancer cells respond to type I collagen by inducing snail expression to promote membrane type 1 matrix metalloproteinase-dependent collagen invasion. J Biol Chem. 2011; 286:10495–10504. [PubMed: 21288898]

32. Froeling FEM, Mirza TA, Feakins RM, Seedhar A, Elia G, Hart IR, Kocher HM. Organotypic culture model of pancreatic cancer demonstrates that stromal cells modulate E-Cadherin, beta-catenin, and Ezrin expression in tumor cells. Am J Pathol. 2009; 175:636–648. [PubMed: 19608876]

33. Yi XP, Han T, Li YX, Long XY, Li WZ. Simultaneous silencing of XIAP and survivin causes partial mesenchymal-epithelial transition of human pancreatic cancer cells via the PTEN/PI3K/Akt pathway. Mol Med Rep. 2015; 12:601–608. [PubMed: 25707849]

34. Yin T, Wang C, Liu T, Zhao G, Zha Y, Yang M. Expression of snail in pancreatic cancer promotes metastasis and chemoresistance. J Surg Res. 2007; 141:196–203. [PubMed: 17583745]

35. Sousa CM, Biancur DE, Wang X, Halbrook CJ, Sherman MH, Zhang L, Kremer D, Hwang RF, Witkiewicz AK, Ying H, Asara JM, Evans RM, Cantley LC, Lyssiotis CA, Kimmelman AC. Pancreatic stellate cells support tumour metabolism through autophagic alanine secretion. Nature. 2016; 536:479. [PubMed: 27509858]
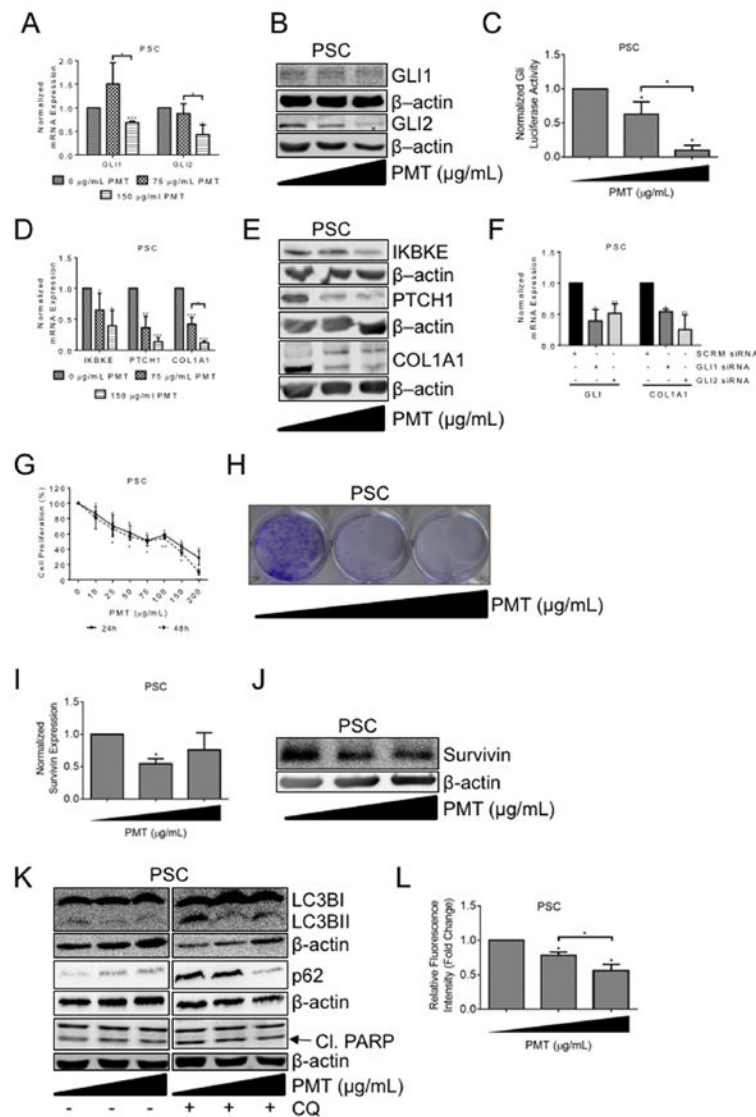
Fig. 1. Palmatine (PMT) modulates cellular homeostasis by inhibiting GLI, survivin, COL1A1 in human pancreatic stellate cells (PSCs)

A–B. Total RNA (A) and whole cell protein extracts (B) prepared from logarithmically growing human pancreatic stellate cells (PSCs) treated with 0, 75, or 150 µg/mL PMT for 24 and 48 h. mRNA expression and protein levels of GLI1 and GLI2 were determined using Real-time PCR and western blotting respectively. β-actin was used as a loading control. C. Logarithmically growing PSCs were transfected with GLI-luciferase reporter (containing 8 GLI binding sites) and Renilla luciferase plasmids. Following 24 h transfection, cells were treated with 75 and 150 µg/mL PMT for additional 24 h and luciferase activity was measured. Firefly luciferase normalized to renilla luciferase is shown. **D–E**. Total RNA (D) and whole cell protein extracts (E) prepared from logarithmically growing PSCs treated with 0, 75, or 150 µg/mL PMT for 24 and 48 h was used to analyze mRNA expression by Real-Time PCR and protein levels by immunoblot analysis of GLI downstream targets including IκBε, PTCH1 and COL1A1. β-actin was used as a loading control. **F**. PSCs were

transfected with scrambled or siRNA specific for GLI 1 or GLI2. 48 h after transfection, total RNA was prepared and used in Real-Time PCR to analyze expression changes of GLI1 and COL1A1. Data presented is an average + sd of three or more independent experiments conducted in triplicate. **G**. Logarithmically growing PSCs were treated with increasing doses of PMT for 24 or 48 h and cell proliferation was measured using MTT assay as described in methods. Data presented is an average + sd of 2 independent experiments conducted in triplicate. **H**. Logarithmically growing PSCs were treated with PMT (50 and 75 μg/mL) for 24 h. Following treatment, cells were washed and media replaced with no PMT. Cells were allowed to grow for 7–10 days and stained with crystal violet to monitor colony formation. Briefly, cells were seeded in 6-well plates at low density (500 cells per well). 24 h later cells were treated with PMT for 24 and 48 h. Following treatment with PMT, cells were washed with PBS and maintained for 7–10 days in complete media till colonies were formed. The colonies were fixed and stained with 1% methanol-crystal violet mixture. A representative picture of three independent experiments is shown. **I–J**. Total RNA (I) and whole cell protein extracts (J) prepared from logarithmically growing PSCs treated with 0, 75, or 150 μg/mL PMT for 24 h was used to analyze Survivin mRNA expression by Real-Time PCR and protein levels by immunoblot analysis. β-actin was used as a loading control. **K**. Whole cell protein extracts prepared from logarithmically growing PSCs treated with 0, 75, or 150 μg/mL PMT for 24 h in the absence or presence of 5 μM chloroquine (CQ) was used to analyze levels of LC3, p62 and cleaved PARP by immunoblot analysis. β-actin was used as a loading control. L. For cell invasion assay, 50,000 PSCs resuspended in serum-free media with or without PMT was added in triplicate to the top chamber of the invasion assay assembly. 150 μl of serum containing media was added to the lower chamber. The plate was incubated at 37 °C overnight. Following 24 h incubation, cells that had migrated to the bottom were lysed using detachment buffer and fluorescence was detected with a fiuorescence plate reader. Data presented is an average + sd of three independent experiments conducted in triplicate. Statistical significance was evaluated using student t-test and p values < .05 was considered significant (* = p   .05, ** = p   .001). Western blots shown are representative blot of three independent immunoblot images. (For interpretation of the references to colour in this figure legend, the reader is referred to the Web version of this article.) Source of antibodies are as follows: GLI2, PATCHED1 (Santa Cruz Biotechnology, Santa Cruz, CA), IKBKE, Survivin, LC3B (Cell Signaling Technology, Beverly MA), p62 (Enzo life Science, Farmingdale, NY), and GLI1 (Thermo Fisher Scientific, Rockford, IL). Odyssey® Infrared Imaging System was used for detecting GLI2 and PTCH1 and IRDye® 800CW and IRDye® 680rd conjugated secondary antibodies (LI-COR Biotechnology, Lincoln, NE) were used. Other proteins were developed using chemiluminescence as previously described. Forward (F) and reverse (R) primer sequences used are:

1.   GLI (F- CTGGATCGGATAGGTGGTCT and R-CAGAGGTTGGGAGGTAAGGA)

2.   GL2 (F-GCCCTTCCTGAAAAGAAGAC and R-CATTGGAGAAACAGGATTGG)

3.   PTCH1 (F- TGACCTAGTCAGGCTGGAAG and R-GAAGGAGATTATCCCCCTGA)

4. COL1A1 (F- AACATGACCAAAAACCAAAAGTG and R-CATTGTTTCCTGTGTCTTCTGG)

5. GAPDH (F- ACCCACTCCTCCACCTTG and R-CTCTTGTGCTCTTGCTGGG)

6. IKBKE Taqman probe HS01063858

7. Survivin Taqman probe Hs00153353

8. GAPDH Taqman probe Hs02758991
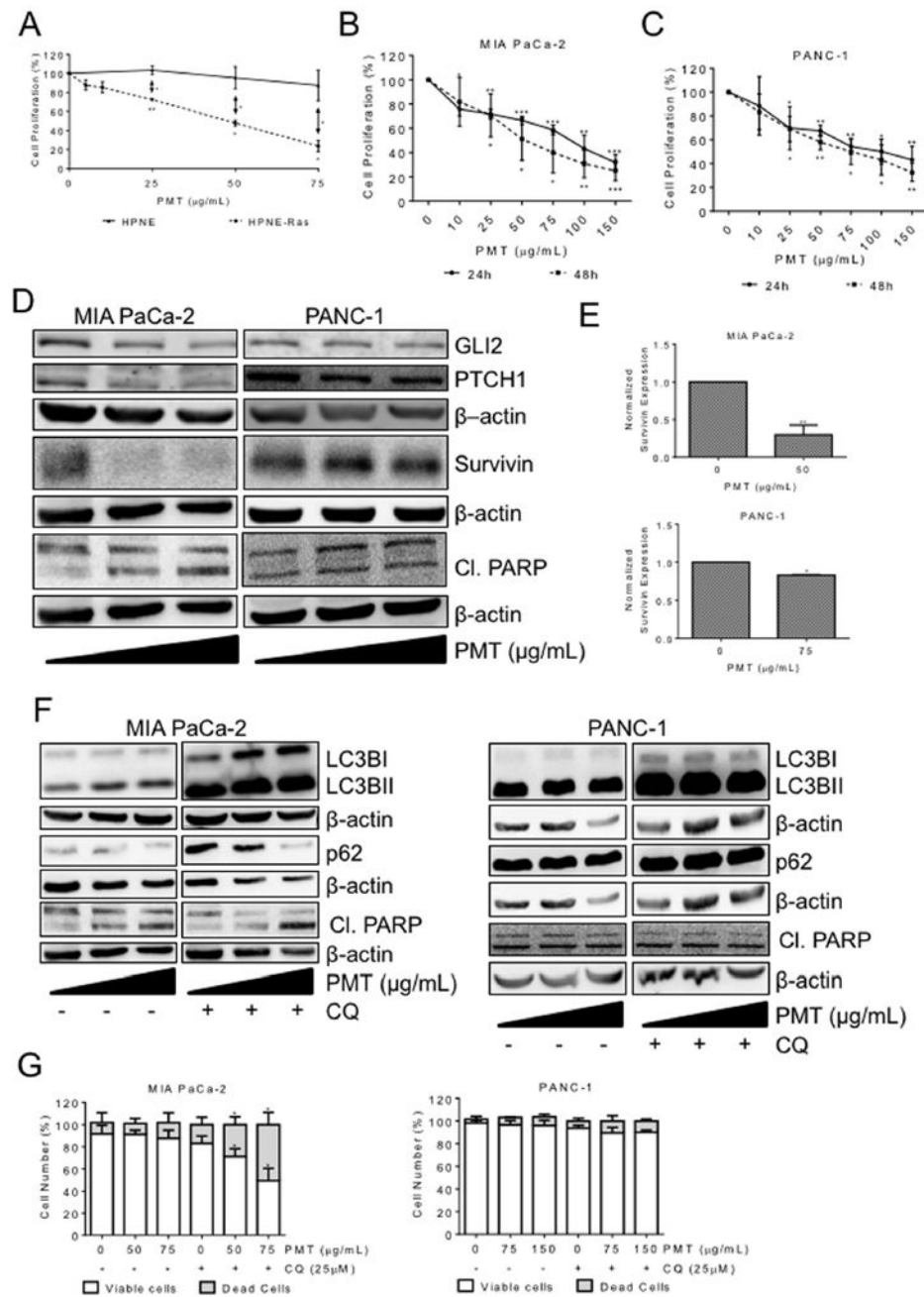
Fig. 2. Palmatine (PMT) inhibits growth of human pancreatic cancer cells through modulation of autophagy

A–C. Logarithmically growing HPNE (n = 3), HPNE-Ras (n = 2), MIA PaCa-2 (n = 3), and PANC-1 (n = 3) were treated with increasing doses of PMT for 24 and/or 48 h and cell proliferation was measured using MTT assay as described in methods. Data presented is an average + sd of 2–3 independent experiments conducted in triplicate. **D–E.** Whole cell protein extracts prepared from logarithmically growing human MIA PaCa-2 (30 h), and PANC-1 (48 h) cells treated with 0, 75, or 150 µg/mL PMT was used to analyze GLI2,

PTCH1, Survivin, Cleaved PARP by immunoblot analysis. β-actin was used as a loading control. Quantification of changes in survivin expression is shown in E. **F–G**. Whole cell protein extracts prepared from logarithmically growing MIA PaCa-2, and PANC-1 cells treated with 0, 75, or 150 μg/mL PMT for 48 h in the absence or presence of 5 μM chloroquine (CQ) to measure autophagic flux. Levels of LC3 and p62 as a measure of autophagy and cleaved PARP as a measure of apoptosis were analyzed using immunoblot analysis (F). β-actin was used as a loading control in immunoblot analysis. Cell viability using trypan blue exclusion assay is shown (G). Data presented is an average ± sd of three independent experiments conducted in triplicate. Statistical significance of the data presented is evaluated using student t-test and p values < .05 was considered significant (* = p   .05, ** = p   .001). Western blots shown are representative blot from three independent immunoblot images.
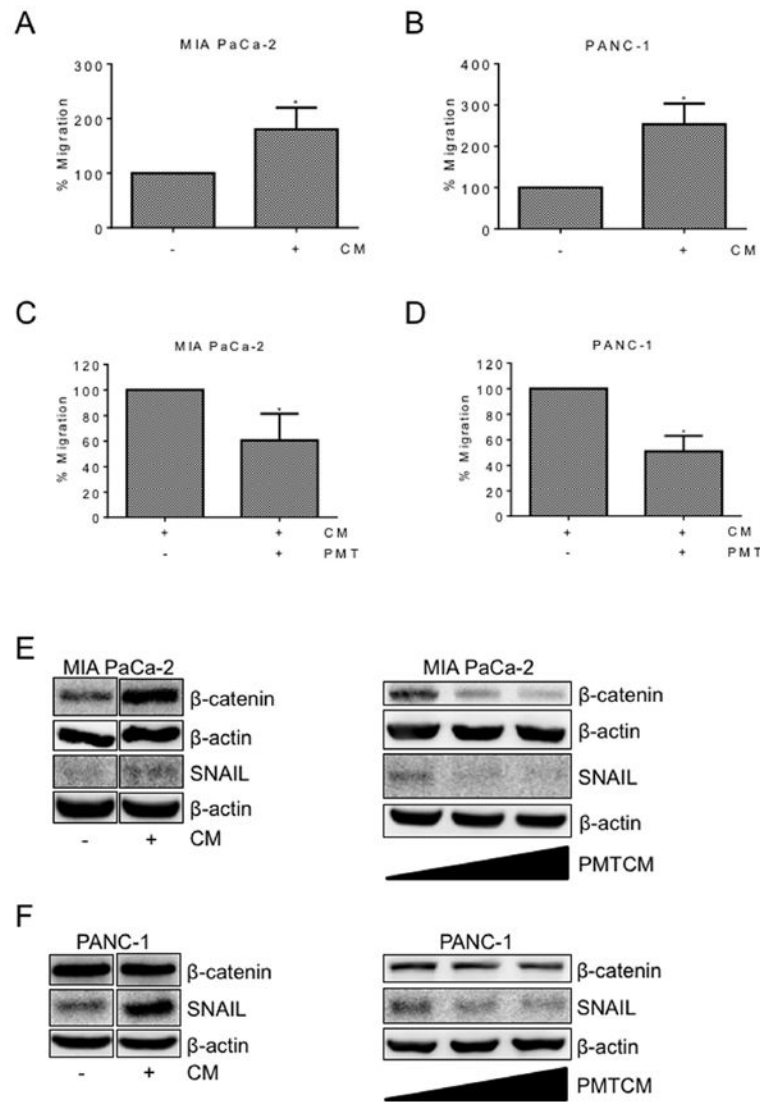
Fig. 3. Palmatine (PMT) inhibits stellate-cancer cell communication

A–D. Conditioned media (CM) generated from PSCs increases migratory ability of pancreatic cancer cells MIA PaCa-2 and PANC-1 cells (A and B) while CM generated from PSCs treated with Palmatine (PMT) reduces their migratory ability (C and D) as evidenced by wound scratch assay. PSCs with 70% confluency were used for generation of CM. The media was then replaced with serum free media containing 25 mM glucose and cells were incubated for 48 h. The supernatant centrifuged for 10 min at 10,000 G to remove debris and stored at −80 °C until use as CM. Serum free CM was used for wound scratch assays. PMT conditioned media (PMT CM) was generated by treating PSCs with PMT in media containing 10% FBS. For wound scratch assays, following attachment of cells, a scratch was made using a 200-μl tip. The wells were then rinsed with PBS and fresh media containing PMT was added. Cells were incubated for 20–24 h and monitored for gap closure using a Zeiss Primo Vert microscope attached to a Sony Camera. Images captured were scanned and distance migrated was measured by a ruler. Percent migration was calculated based on

distance migrated by untreated cells, which was set at 100%. Data presented is an average ± sd of 3 independent experiments conducted in triplicate. **E–F**. Whole cell protein extracts prepared from MIA PaCa-2, and PANC-1 cells growing with CM generated from PSCs (left panel E and F) or CM generated from PSCs treated with PMT (75, or 150 μg/mL) for 24 and 48 h was used to analyze protein levels of SNAIL and β-catenin by immunoblot analysis. β-actin was used as a loading control. All data presented was derived from three individual experiments. WB images are representative images. (* = p   .05).

A

Sub Pathway	Biochemical Name	GLM/GRM
Glutamate Metabolism	glutamate	2.68
	glutamine	1.91
Glycolysis	glucose	0.19
	pyruvate	0.45
	lactate	0.94
	glycerate	0.6
Pentose Metabolism	ribose	0.69
	ribitol	0.85
	xylonate	1.11
	xylitol	1
TCA Cycle	citrate	1.13
	alpha-ketoglutarate	0.55
	succinate	0.91
	fumarate	0.76
	malate	1.04

B

| Sub Pathway	Biochemical Name	GLM/GRM
Glutamate Metabolism	glutamate	0.96
	glutamine	2.2
Glycolysis	glucose	0.01
	glucose 6-phosphate	0.02
	glucose 1-phosphate	0.61
	fructose-6-phosphate	0.05
	Isobar: fructose 1,6-diphosphate, glucose 1,6-diphosphate, myo-inositol 1,4 or 1,3-diphosphate	0.04
	dihydroxyacetone phosphate (DHAP)	0.01
	1,3-dihydroxyacetone	0.26
	3-phosphoglycerate	0.26
	phosphoenolpyruvate (PEP)	0.2
	pyruvate	1.43
	lactate	0.57
	glycerate	0.49
Nucleotide Sugars, Pentose Metabolism	6-phosphogluconate	0.19
	ribose 5-phosphate	0.09
	ribulose/xylulose 5-phosphate	0.12
	ribulose	0.14
	ribose	0.13
	ribitol	0.62
	xylonate	0.7
	xylitol	0.48
	arabitol	0.8
	UDP-glucose	1.31
	UDP-glucuronate	0.69
TCA Cycle	citrate	1.05
	alpha-ketoglutarate	2.33
	succinate	0.78
	fumarate	0.98
	malate	0.79

Fig. 4. Identification of glutamine and glucose as secretory factors involved in stellate cancer cell communication

Heat maps and representative box plots of secretory (A) and intracellular (B) metabolites. In the heat map, numerical values indicate relative fold change for the given comparison. Red (p .05) boxes represent significantly increased biochemicals. Green (p .05) boxes represent significantly decreased biochemicals. Pink and light green boxes represent biochemicals that are trending (.05 < p < .10) up or down, respectively. (For interpretation of the references to colour in this figure legend, the reader is referred to the Web version of this article.)
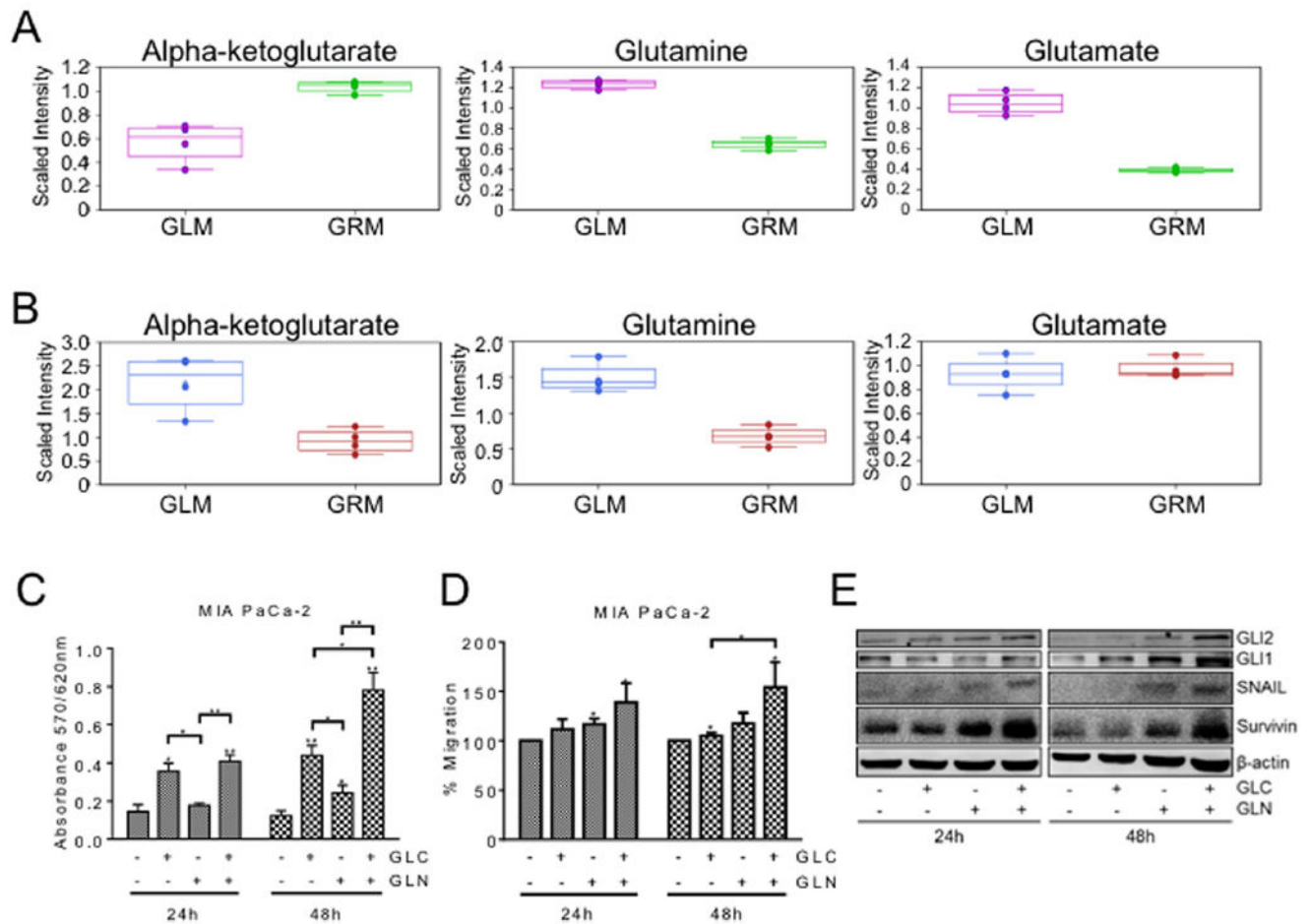
Fig. 5. Palmatine (PMT) inhibits Glutamine mediated effects in MIA-PaCa-2 cells derived from primary tumor and CFPaC-1 cells derived from liver metastasis

A–B. Box plots are used to convey the spread of the three key metabolites (α-ketoglutarate, glutamine and glutamate) with the middle 50% of the data represented by the shaded boxes and the whiskers reporting the range of the data. The solid bar across the box represents the median value of those measured while the + is the mean. Data are scaled such that the median value measured across all samples was set to 1.0. Any outliers are shown as dots outside the whiskers of the plot. Panel A and B represents secretory and intracellular metabolites respectively. **C–D**. Logarithmically growing MIA PaCa-2 cells were treated with 10 mM glucose (GLC) or 2 mM glutamine alone (GLN) or in combination was used to determine proliferative© and migratory (**D**) ability following 24 and 48 h incubation. Data presented is an average + sd of 3 independent experiments conducted in triplicate. **E**. Whole cell extracts prepared from MIA PaCa-2 cells treated with 10 mM glucose (GLC) or 2 mM glutamine alone (GLN) or their combination for 24 and 48 h. Changes in levels of GLI1, GLI2, SNAIL and Survivin were determined by immunoblot analysis. β-actin was used as a loading control.
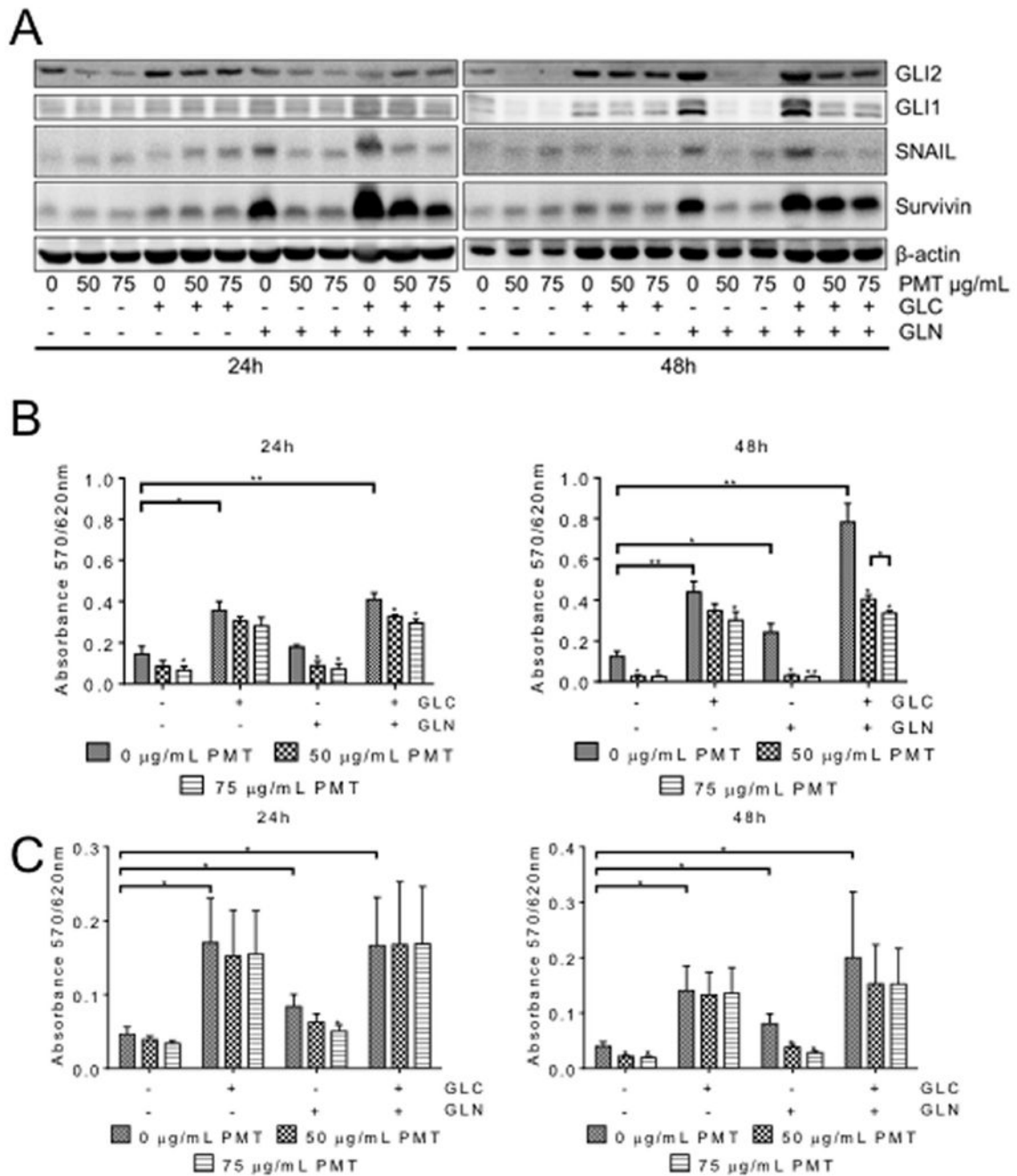
Fig. 6. Palmatine (PMT) inhibits Glutamine mediated effects in MIA-PaCa-2 cells

A. Logarithmically growing MIA PaCa-2 cells were treated with 10 mM glucose (GLC) or 2 mM glutamine alone (GLN) or their combination in the presence and absence of PMT (50 and 75 μg/mL). 24 and 48 h after treatment, whole cell extracts were prepared to analyze changes in levels of GLI1, GLI2, SNAIL and Survivin by immunoblot analysis. β-actin was used as a loading control. All data presented was derived from three individual experiments. WB images are representative images. (* = p   .05). **B**. Logarithmically growing MIA PaCa-2 cells were treated with 10 mM glucose (GLC) or 2 mM glutamine alone (GLN) or

their combination in the presence and absence of PMT (50 and 75 μg/mL). MTT assay was used to determine proliferation. Data presented is an average ± sd of 3 independent experiments conducted in triplicate. All data presented was derived from three individual experiments. WB images are representative images. (* = p ≤ .05). **C**. Logarithmically growing CFPaC-1 cells were treated with 10 mM glucose (GLC) or 2 mM glutamine alone (GLN) or their combination in the presence and absence of PMT (50 and 75 μg/mL). MTT assay was used to determine proliferation. Data presented is an average ± sd of 3 independent experiments conducted in triplicate. All data presented was derived from three individual experiments. WB images are representative images. (* = p ≤ .05).
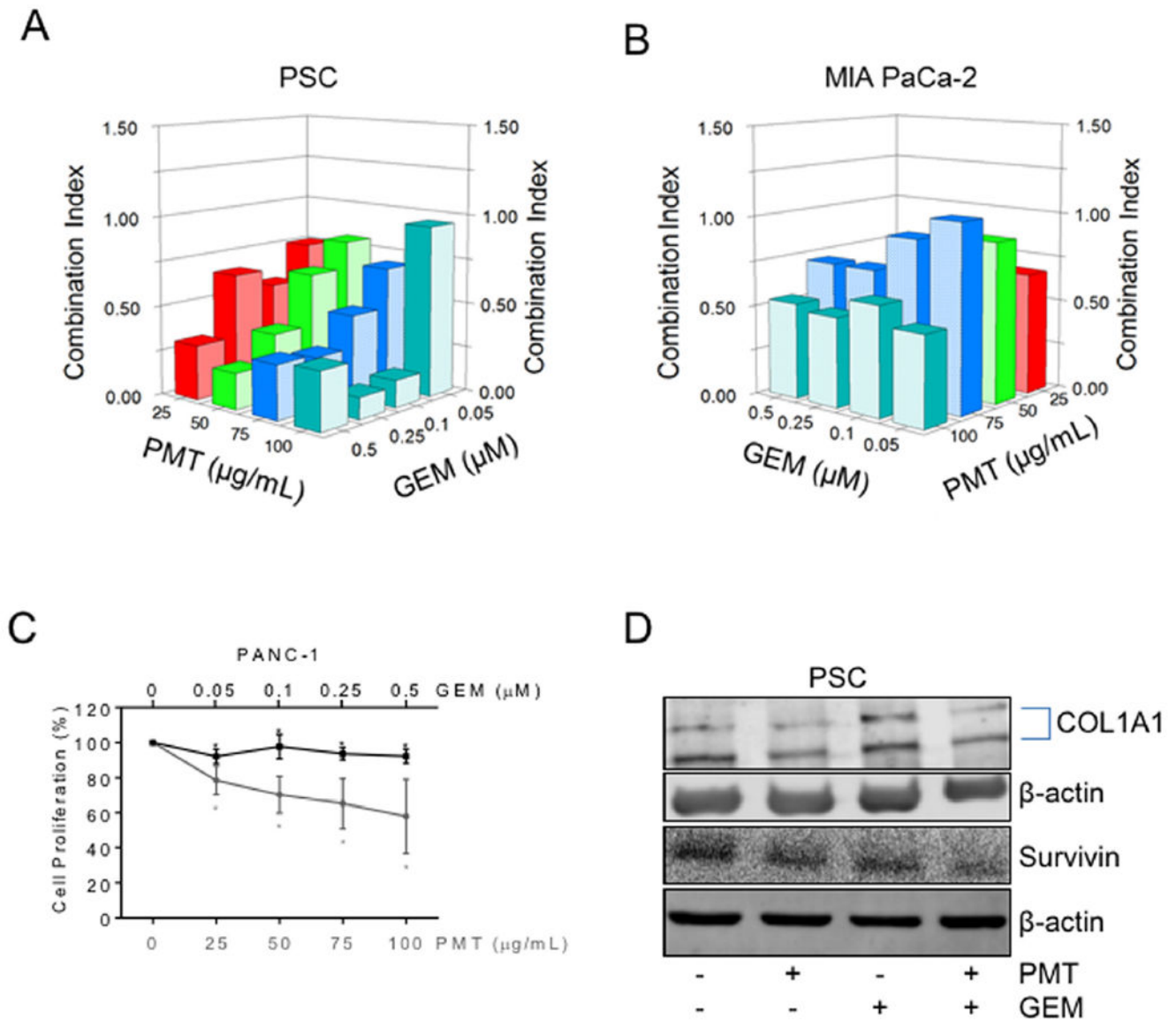
Fig. 7. PMT potentiates gemcitabine (GEM) activity in PSCs and MIA PaCa-2 cells

A–B. PMT potentiates GEM-mediated growth inhibition in PSCs (**A**) and in MIA PCa-2 (**B**) cells. Respective cells were treated with increasing concentrations of PMT (0, 25, 50, 75 and 100 μg/mL), Gemcitabine (GEM; 0, 0.05, 0.1, 0.25, 0.5 μM), or a combination of both PMT and GEM. 24 h later, cell proliferation was measured using MTT assay. Combination index analysis was used to calculate combinatorial growth inhibitory activity essentially as described in methods. A representative CI data from three independent experiments for each cell line conducted in triplicate is shown. **C**. PMT alone inhibits proliferation of PANC-1 cells but does not potentiate Gemcitabine (GEM) activity. Experimental details are essentially similar to panel A. **D**. Logarithmically growing PSCs were treated with 25 μg/mL PMT alone, 0.1 μM GEM or combination of both PMT and GEM (doses that ware synergistic). 24 h later whole cell extracts were prepared and examined for changes in

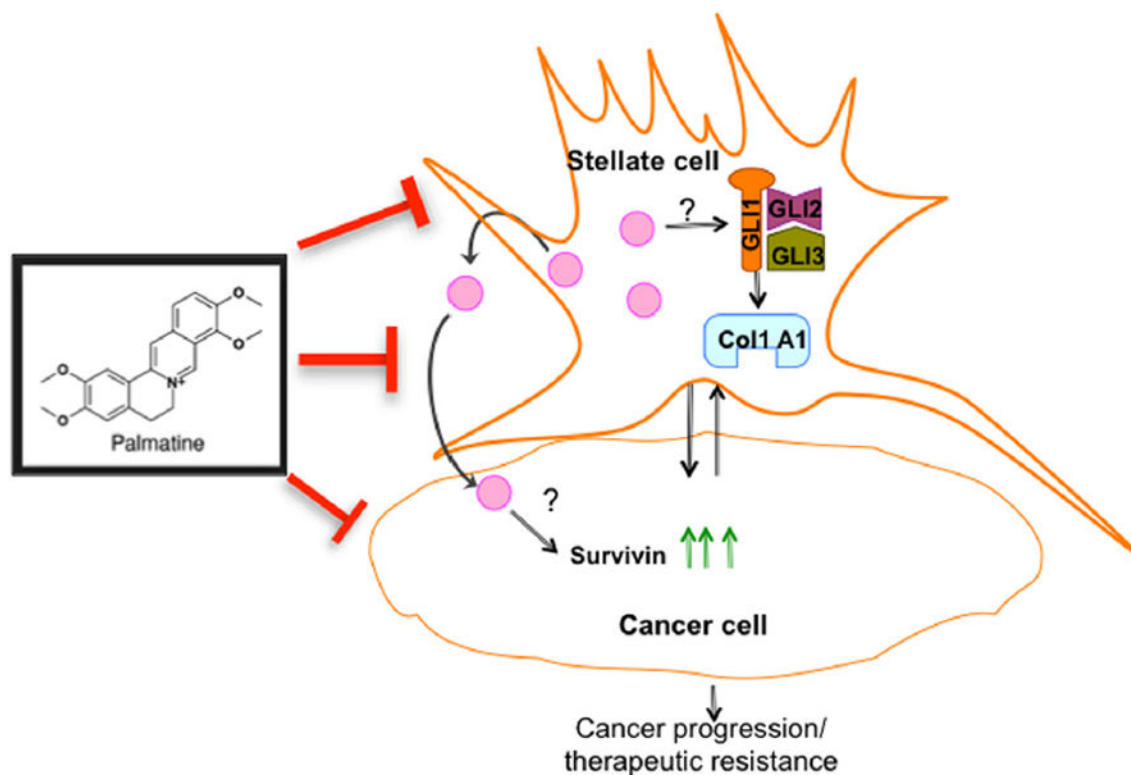COL1A1 and Survivin proteins by immunoblot analysis. β-actin was used as a loading control. A representative immunoblot from three independent experiments is shown.

Fig. 8. Hypothetical model

In the tumor microenvironment glutamine secreted from stellate cells activates cancer cell survival possibly by up regulating Survivin. Glutamine also up regulates COL1A1 transcriptionally via GLI in stellate cells leading to collagen accumulation. Palmatine inhibits GLI/COL1A1 in stellate cells and Survivin in cancer cells. Further, palmatine inhibits glutamine mediated stellate-cancer cell communication. These events possibly contribute to growth inhibition and sensitivity to gemcitabine. Pink circles represent glutamine. (For interpretation of the references to colour in this figure legend, the reader is referred to the Web version of this article.)

Table 1

Alteration in the levels of secreted and intracellular metabolites in PSCs.

Media ANOVA Contrasts	Total number of biochemicals with p ≤ .05	Increased or decreased levels of secreted metabolites)
GLM/GRM	60	20 increased/40 decreased
Cells	Total number of biochemicals with p ≤ .05	Increased or decreased levels of intracellular metabolites)
ANOVA Contrasts		
GLM/GRM	164	44 increased/120 decreased

GLM: PSCs grown in low glucose media (5 mM).
GRM: PSCs grown in glucose rich media (25 mM).
Only significantly altered levels of metabolites shown.